Biochimica et Biophysica Acta 1848 (2015) 554–560

Contents lists available at ScienceDirect

Biochimica et Biophysica Acta

journal homepage: www.elsevier.com/locate/bbamem

Monitoring antibacterial permeabilization in real time using time-resolved flow cytometry

João Miguel Freire [a,1], Diana Gaspar [a,1], Beatriz Garcia de la Torre [b], Ana Salomé Veiga [a], David Andreu [b], Miguel A.R.B. Castanho [a,*]

[a] Instituto de Medicina Molecular, Faculdade de Medicina, Universidade de Lisboa, Av. Prof. Egas Moniz, Lisbon 1649-028, Portugal
[b] Department of Experimental and Health Sciences, Pompeu Fabra University, Barcelona Biomedical Research Park, Barcelona E-08003, Spain

ARTICLE INFO

Article history:
Received 27 June 2014
Received in revised form 13 October 2014
Accepted 4 November 2014
Available online 10 November 2014

Keywords:
Time-resolved flow cytometry
Antimicrobial peptide
Live/dead assay
Peptide–lipid interaction
Antimicrobial action
Lipopolysaccharide

ABSTRACT

Despite the intensive study of antibiotic-induced bacterial permeabilization, its kinetics and molecular mechanism remain largely elusive. A new methodology that extends the concept of the live–dead assay in flow cytometry to real time-resolved detection was used to overcome these limitations. The antimicrobial activity of pepR was monitored in time-resolved flow cytometry for three bacterial strains: *Escherichia coli* (ATCC 25922), *E. coli* K-12 (CGSC Strain 4401) and *E. coli* JW3596-1 (CGSC Strain 11805). The latter strain has truncated lipopolysaccharides (LPS) in the outer membrane. This new methodology provided information on the efficacy of the antibiotics and sheds light on their mode of action at membrane-level. Kinetic data regarding antibiotic binding and lytic action were retrieved. Membrane interaction and permeabilization events differ significantly among strains. The truncation of LPS moieties does not hamper AMP binding but compromises membrane disruption and bacterial killing. We demonstrated the usefulness of time-resolved flow cytometry to study antimicrobial-induced permeabilization by collecting kinetic data that contribute to characterize the action of antibiotics directly on bacteria.

1. Introduction

Most gold-standard methods used to study the efficacy of antibiotics are time consuming and provide limited information on the kinetics of bacterial killing or inactivation, which hampers retrieving information that may be useful to deduce the molecular mechanisms involved. The permeabilization/killing kinetics provides valuable information on the molecular mode of action, target and specificity of the antibiotic. In this study, we describe a methodology that automatically detects the kinetics of antibiotic-induced bacterial permeabilization. This methodology uses a commercially available mixture of two dyes (Syto-9 and Propidium iodide [PI]) that allows to quantify the fraction of dead bacterial cells in a population [1,2] using time-resolved flow cytometry. The action of pepR, an antimicrobial peptide (AMP) developed in our labs, against *Escherichia coli* was studied through the application of the method. AMPs are small, structurally diverse and usually cationic amphipathic peptides that interact directly with lipids [3–6] permeabilizing Gram-positive and Gram-negative bacteria including drug-resistant strains [7,8], although few exceptions have been reported [4,6,7]. By targeting membranes, AMPs induce a rapid death in bacterial cells with low chances for resistance development [4,6,7]. The fast kinetics of permeabilization is a very demanding technical challenge that has to be specifically addressed when aiming at time-resolved data.

Altogether, this work describes and characterizes a novel and robust technique, time-resolved flow cytometry, to evaluate the antimicrobial effect of AMPs, which may be extended to other membrane-targeting antibiotics or to evaluate cellular cytotoxicity. The kinetic detail obtained with this technique may help to contribute to clarify the mode-of-action of antibiotics against different bacterial species and mutant bacteria. Gaining deeper insights on the mode of action of antibacterial agents may lead to a more rationally guided drug design, which is extremely important to avoid the emergence of multi-drug-resistant bacterial strains as a consequence of antibiotic misuse [3,9,10].

2. Materials and methods

2.1. Materials

4-(2-Hydroxyethyl)piperazine-1-ethanesulfonic acid (HEPES), and sodium chloride (NaCl) were purchased from Merck Millipore (Darmstadt, Germany). Luria-Bertani agar was from Applichem LiveScience (Darmstadt, Germany), LB broth from Fisher Scientific (Waltham, MA, USA) and isopropyl alcohol from VWR BDH Prolabo (Leicestershire, England). LIVE/DEAD *Bac*Light Bacterial Viability Kit,

Abbreviations: AMP, antimicrobial peptide; FRET, Förster resonance energy transfer; PI, propidium iodide; LPS, lipopolysaccharide

* Corresponding author. Tel.: +351 217985136; fax: +351 217999477.
E-mail address: macastanho@medicina.ulisboa.pt (M.A.R.B. Castanho).

[1] The authors contributed equally to this work.

http://dx.doi.org/10.1016/j.bbamem.2014.11.001
0005-2736/

for quantitative assays (L7012) was purchased from Life Technologies (Carlsbad, CA, USA). Dengue virus strain 2-derived peptide pepR (LKRWGTIKKSKAINVLRGFRKEIGRMLNILNRRRR-amide) was synthesized by solid-state synthesis as described elsewhere [11]. pepR stock solution (500 μM) was prepared in sterile Milli Q water. All other laboratory used reagents were of the highest quality available commercially. All the experiments were performed at pH 7.4 at 22 °C ± 1 °C.

2.2. Methods

2.2.1. Preparation and culture of bacterial strains

The *E. coli* strains used for the studies were ATCC 25922, K-12 wild-type (*wt*) (CGSC Strain 4401) and JW3596-1 (CGSC Strain 11805) [12,13], from now on abridged as 25922, K-12*wt* and JW3596-1, respectively. Bacteria were maintained as stock cultures at −80 °C and revived by growing on Luria–Bertani agar plates overnight at 37 °C. For each bacterial strain, two suspensions with 10^8 cfu/mL were prepared in LB broth by direct suspension of colonies to minimize stress conditions until experimental procedures. Bacterial suspensions were then centrifuged for 10 min at 4000 ×g twice and resuspended in either HEPES buffer, pH 7.4, containing 150 mM NaCl, for live bacteria, or in HEPES buffer after the first centrifugation and 70% isopropyl alcohol after the second centrifugation to induce bacterial death. The suspensions for live and dead bacteria were afterward incubated at room temperature for 1 h, mixing every 15 min. One final centrifugation was performed and bacteria were resuspended in HEPES buffer. All bacterial suspensions were diluted in HEPES buffer to 10^6 cfu/mL.

2.2.2. Bacterial live/dead assay using flow cytometry

Flow cytometry experiments were performed using a BD LSR Fortessa from BD Biosciences (San Jose, CA, USA), which is equipped with 3 lasers (violet—405 nm, blue—488 and red—640 nm), forward and side scatter detectors and 9 fluorescence emission detectors (530/30 and 695/40 channels were used for Syto-9 and PI detection, respectively). The Live/Dead kit assay is composed of two fluorescent dyes, Syto-9 and PI. Syto-9 translocates cell membranes being able to complex with bacterial DNA; in contrast, PI is only able to interact with bacterial DNA if the lipid bilayer is damaged, indicating that PI-positive bacteria are fragilized or dead. The kit assay used to evaluate the antimicrobial activity of pepR on *E. coli* was obtained from Life Technologies (L7012) and bacterial stains were performed according to the manufacturer's instructions. Briefly, 1.5 μL of both Syto-9 and PI was added at each test tube with 1 mL of bacterial suspension (10^6 cfu/mL). For laser calibration purposes and gating selection, unstained and single-stained Syto-9 or PI Live and Dead bacteria were also recorded, and a standard curve for bacterial death detection with Live/Dead staining was plotted (Fig. 1) [2,14].

2.2.2.1. Steady-state flow cytometry. For the pepR antimicrobial activity assays against 25922, K-12*wt* and JW3596-1, concentrations of pepR up to 20 μM were added to 1 mL of a bacterial suspension at 10^6 cfu/mL labeled with both Syto-9 and PI. The mixture was incubated for 1 h, and 15,000 events were recorded from each solution (three independent assays were performed for each condition). The percentage of dead bacteria in each solution was calculated according to Eqs. (1) and (2) in Section 3.

2.2.2.2. Time-resolved flow cytometry. In the kinetic acquisition mode, the Syto-9 and PI channels of the 10^6 cfu/mL bacterial suspensions were recorded for 60 min immediately after addition of 20 μM pepR (Fig. 2, Figs. S1 and S2). The average fluorescence intensities $\langle I_{f,g}\rangle$ and $\langle I_{f,r}\rangle$ of the events recorded at each time point, t, was calculated. Due to AMP activity, as bacterial permeabilization progresses, the average fluorescence signal of Syto-9 ($\langle I_{f,g}\rangle$) decreases and $\langle I_{f,r}\rangle$ increases [15] (Fig. 2B). The ratio between both signals (R, Eq. (2)) can be directly correlated to the % of cell death if one normalizes for a 0%–100% ($a - b$) fluorescence ratio interval (Eq. (1)). Performing this procedure over time, one calculates the evolution of the percentage of bacterial death over time induced by the antibiotic (Fig. 2C), $R(t)$. The $R(t)$ of a bacterial suspension with no addition of pepR was also calculated to account for natural bacterial death during the 60 minutesmin of experiment and for additional unspecific fluorescence signal background correction. During the 60 min, the number of viable cells did not change (Supp. Fig. S3 – —green circles and Supp. Video S1).

2.2.3. Zeta-potential of bacteria

Zeta potential studies were performed in a Zetasizer Nano ZS (Malvern instruments, Worcestershire, UK) equipped with a 633-nm HeNe laser using disposable Zeta cells with gold electrodes. The protocol used was adapted from Alves et al. [11] to ensure optimal measurement conditions for the different *E. coli* strains. Briefly, the bacteria cells were suspended in filtered HEPES buffer at 10^7 cfu/mL, dispensed into the disposable zeta cells and allowed to equilibrate for 15 min at 25 °C before measuring. The experiments were carried out in two different days using independently grown cultures ($n > 3$). Measurements were repeated in the same conditions with the addition of 20 μM pepR.

2.2.4. Data analysis

The experimental values of % dead bacteria are calculated from Eq. (1) and plotted over time. Eqs. (3) and (4) are then combined to fit the data and retrieve k_0, k_2 and f. These parameters contain information on cooperativity (f), kinetics of binding of the antibiotics to bacterial targets (k_0) and kinetics of killing (k_2). Data fitting analysis was performed with GraphPad Prism software v5.0. Mean ± SD from 3 independent experiments for each condition is represented. The validation of the fitting models was achieved by an extra sum-of-squares F-test in order to choose the simplest model to describe the antimicrobial action against the bacteria tested ($p < 0.01$) between fittings with Eqs. (3) and (S12) (see supporting information for more detail). The goodness of the fit was analyzed with R^2, sum-of-squares and residual plot analysis with normality test (D'Agostino-Pearson test with $p < 0.0001$) (Supplementary Section 3, Fig. S3).

3. Theory

Syto-9 is a green-fluorescent (510–540 nm) nucleic acid stain that is able to penetrate both healthy and damaged bacterial cells. After incubation with Syto-9, virtually all bacteria emit green fluorescence upon excitation with blue light enabling counting total cells. In contrast, PI is unable to penetrate healthy bacteria. Its red emission (620–650 nm) is only associated to permeabilized bacteria (Fig. 1A). When both dyes are present in the same cell, the emission of Syto-9 is decreased due to the displacement of one stain by the other and apparent quenching by Förster resonance energy transfer (FRET) [15]. The emission spectra of bacterial suspensions may be integrated in the 510–540 nm and 620–650 nm intervals and the ratio of the corresponding values is compared to a calibration curve obtained with isopropyl alcohol-killed bacteria to calculate the percentage of permeabilized bacteria [15] (Fig. 1B). Although this assay provides useful information on antibiotic efficacy, it does not enable retrieval of kinetic information. Application of these principles to flow cytometry is currently based on steady-state conditions [15] and dependent on user-defined population gating [16]. Nevertheless, flow cytometry allows the analysis of thousands of single events in minutes and detects the evolution of a spectroscopic signal over time [17–20]. Despite this potential, the application of flow cytometry to kinetic studies has been overlooked and the applications described in the literature are limited to the detection of Ca^{2+} intracellular flux [20]. We have used the time-resolved capabilities of flow cytometry to evaluate bacterial susceptibility to antibiotics over time using the fluorescent dyes Syto-9 and PI. Briefly, when a cell passes through the excitation beam, the following data is registered: time since the experiment started, fluorescence intensity in detector 1 ("green," 530/30 BP), fluorescence intensity in detector 2 ("red," 695/40 BP) and forward/side scatter (Fig. 2A). The data are grouped according to regular time intervals (typically 1 s),

and the fluorescence intensity signals of the events in that time-interval are averaged (Fig. 2A). The ratio of the fluorescence intensities (green/red) over time correlates with the bacteria death (Fig. 2B). With proper calibration curve and fitting models, the kinetics of antibiotic-induced bacterial killing can be quantitatively described (Figs. 1C and 2C).

3.1. Calculation of the fraction of permeabilized bacteria

As shown in Fig. 2, $t = 0$ is set at the instant of addition of an antibiotic to a bacterial cells suspension. The ratio of the fluorescence intensities over time relates to the permeabilization of bacteria (Figs. 1B and 2B) according to Eq. (1).

$$\rho_D = \frac{Y(K-1)}{(K-Y)}, \quad Y = 1-\frac{R-b}{a-b} \tag{1}$$

ρ_D is the fraction of permeabilized bacteria. R is the ratio of the average fluorescence intensities of Syto-9 ($\langle I_{f,g}\rangle$) and PI ($\langle I_{f,r}\rangle$) emission after gating, and a and b are the experimental values of R for bacterial populations that are 0% and 100% dead, respectively:

$$R = \frac{\langle I_{f,g}\rangle}{\langle I_{f,r}\rangle} \tag{2}$$

Y is the experimental estimator for the fraction of permeabilized bacteria (ρ_D) and K is an empirical parameter valid for each experiment setup that accounts for the magnitude of the deviations between Y and ρ_D. K is calculated from a calibration curve Y vs. ρ_D using mixtures of known composition of dead and live bacteria (Fig. 1B). If no deviations exist (linear calibration curve), $K \gg 1$ and $Y = \rho_D$. In the case of the experimental setup used in the present study, $K = 2.041$ or 204.1 in a percentual scale (Fig. 1B). The 100% death scale value is set with an assay using bacteria killed with isopropyl alcohol (Figs. 1 and 2B, C).

R is calculated for each time interval, and the fraction of permeabilized bacteria, ρ_D, is calculated over time (Eq. (1)). Fig. 1 illustrates the main sequence of steps in FACS data treatment: (1) raw data (Fig. 2A) analysis and (2) determination of the corrected fraction of dead bacteria (Fig. 1B). The relevance of correcting the estimated fraction of dead bacteria (i.e., conversion of Y into ρ_D – Eq. (1) and Fig. 2B) in kinetic curves is highlighted in Fig. 1C. The calculation of Y from the raw data is described with special attention in supplementary material Section 1 (Fig. S1). For each bacteria strain, a calibration curve (Fig. 1B) is required. Syto-9 and PI binding to bacteria DNA may give different fluorescence intensity signals and thus different R values for each proportion between live and dead/permeabilized bacteria. After proper signal correction (Fig. 1 and Fig. S1), it is possible to estimate the % of live or dead bacteria over time (Fig S1). The evolution of the fraction of dead/permeabilized bacteria over time and its maximum attained value will be dependent on the concentration of the antibiotic administrated. For instance, 100% bacterial death is achieved if concentrations above the MIC value are used, 50% death is expected with [antibiotic] = MIC_{50} and values below 50% of bacterial death/permeabilization are expected when using [antibiotic] ≪ MIC as simulated with pepR titration in Fig. S1 (bottom right panel), using sub-MIC, MIC and over-MIC concentrations showed by the life/dead panels in Fig. S2.

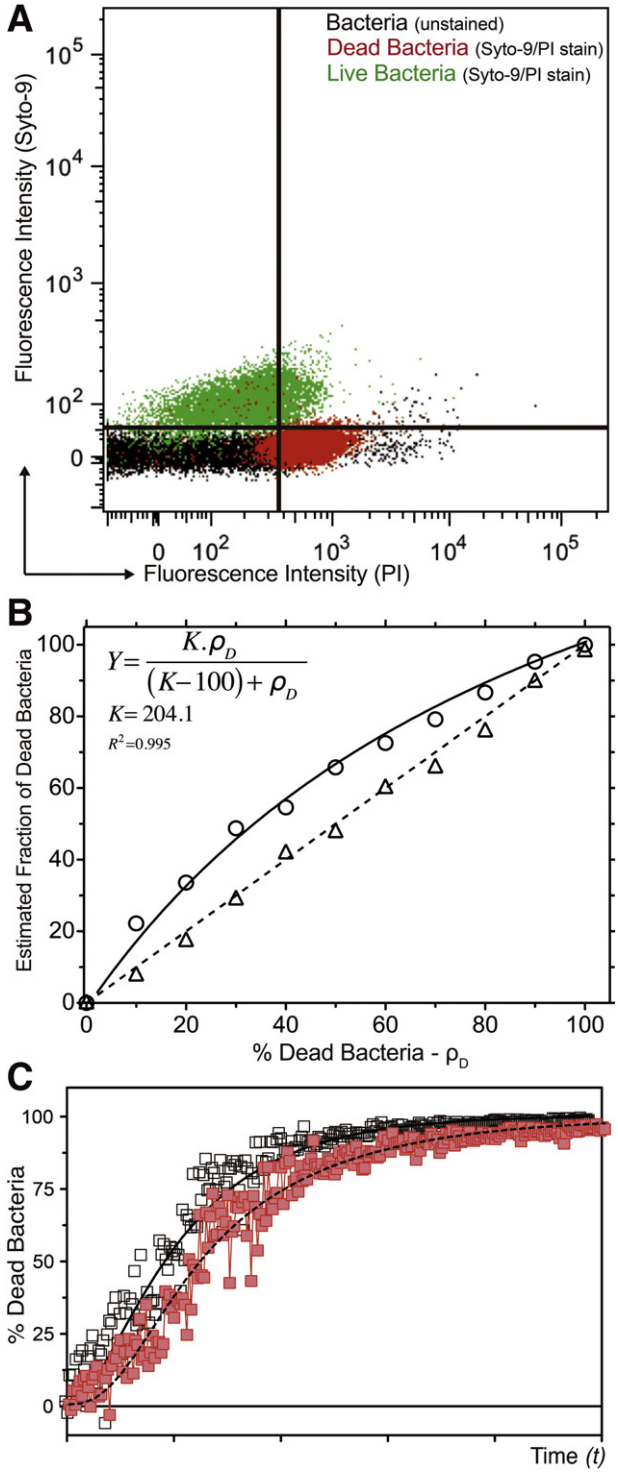

Fig. 1. Main steps in data analysis. (A) Flow cytometry fluorescence correlogram of both fluorescent dyes, Syto-9 and PI for unstained (black), 100% live (green) and 100% dead (red) bacteria. *Escherichia coli* (ATCC 25922) death was induced by isopropyl alcohol. The gatings of Syto-9^+ and PI^+ are represented by solid black lines. (B) The percentage of dead *E. coli* (ATCC 25922) in suspensions of live bacteria and bacteria previously killed with isopropyl alcohol was estimated using the fraction of population in each gate (triangles), or using Eqs. (1) and (2) (white circles). This approach is based on the Syto-9 and PI fluorescence intensity ratio. A deviation from linearity occurs. The uncorrected estimated fraction of dead bacteria in this case (Y in Eq. (1)) is related to the real fraction of dead bacteria (ρ_D) by a rectangular hyperbola (K is an instrumental constant). The black solid line is the result of fitting the experimental data (circles) with a rectangular hyperbolic function ($K = 204.1$). C) The conversion of Y (uncorrected estimate of the fraction of dead bacteria) into ρ_D is of extreme importance as the kinetics of bacterial permeabilization are severely affected. A comparison of the kinetics of permeabilization using uncorrected (grey) and corrected (red) percentage of damaged *E. coli* (ATCC 25922) kinetic curves is shown. The result of fitting Eq. (3) to the data is also shown (solid and dashed line). The corrected curve significantly deviates from the uncorrected curve.

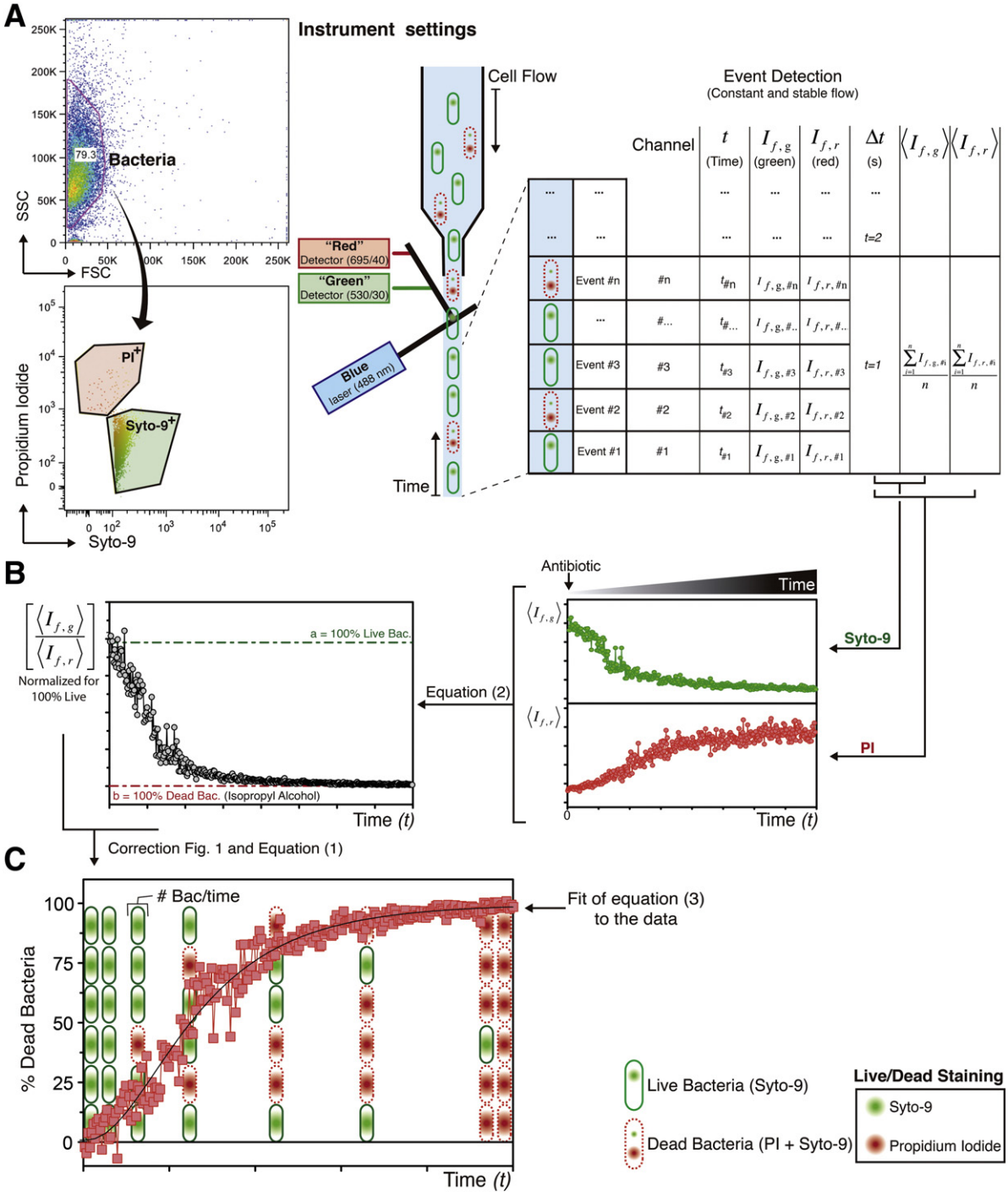

Fig. 2. Workflow of the live/dead assay using time-resolved flow cytometry. (a) *Left panel:* Example of bacterial scatter correlogram (FSC-SSC plot) and population gating selection (*top*) and fluorescence correlogram of Syto-9 and PI, highlighting the LIVE/DEAD gates to identify Syto-9 and PI positive cells (green and red gate, respectively). This example consists in Ec25922 100% live. *Right panel:* Schematic representation of the detection of each bacterial event by the flow cytometry instrument. On a continuous flow, a suspension of bacteria (10^6 cfu/mL) labeled with both Syto-9 (green dot) and PI (red dot) passes through the detection chamber, which is irradiated by a blue laser (488 nm). For each cell passing through the laser beam the forward and side scatter signals are triggered and the order of the event is registered, #, as well as the time in which it occurred, $t_{\#}$. The green fluorescence emission of Syto-9 (530/30 nm) and the red fluorescence from PI (695/40 nm), $I_{f,g,\#}$ and $I_{f,r,\#}$, respectively, are recorded by each detector. Finally, for a pre-defined time interval, Δt (1 s, for instance) the average fluorescence intensity, $\langle I_f \rangle$ (green and red) are determined. (b) For long-period acquisitions and recordings, the average fluorescence intensity can be plotted over time. Immediately after antibiotic addition, one can follow the evolution of both Syto-9 and PI average intensity, $\langle I_{f,g} \rangle$ and $\langle I_{f,r} \rangle$, respectively, over time (green and red plots, respectively—*right panel*). The ratio between the green and red signals, $R(t) = \langle I_{f,g} \rangle (t) / \langle I_{f,r} \rangle (t)$ is related to the evolution of the live bacterial population over time (*left panel*). Using the experimental value of R for 100% live bacteria (green dashed line—*a*) and 0% live bacteria (red dashed line—*b*), it is possible to calculate the % of dead bacteria over time due to the antimicrobial action. (c) The evolution of dead/permeabilized bacteria over time can be calculated from Eq. (1) and the antimicrobial action can be described using Eq. (3), from which one can quantitatively describe the antimicrobial dynamics of the antibiotic under study.

3.2. Kinetic model and data treatment

Assuming for the sake of simplicity that permeabilization leads to death, the kinetics of bacterial death may be described in theoretical terms by the action of an antibiotic, A, that interacts with live bacteria, B_L, which is then converted into dead bacteria, B_D. Assuming that both binding and killing steps are irreversible and A has a defined stoichiometry when binding to B_L:

$$B_L + nA \xrightarrow{k_1} BA_n \xrightarrow{k_2} B_D A_n$$

In excess of A, Eq. (3) [21] applies (additional details in supplementary material Section 2):

$$\rho_D = \frac{[B_D A_n]}{[B_D A_n]_0} = 1 + \frac{k'_1 e^{-k_2 t} - k_2 e^{-k'_1 t}}{k_2 - k'_1}, \quad k'_1 = k_1 [A]^n \tag{3}$$

where $[B_L]_0$ is the concentration of B_L at $t = 0$. Considering that k'_1 may be time-dependent to account for cooperativity on the binding of A to B_L

$$k'_1 = k_0 t^f \tag{4}$$

where k_0 is an empiric fundamental constant and f describes cooperativity ($f < 0$, negative cooperativity; $f > 0$, positive cooperativity; $f = 0$, no cooperativity).

The experimental values of ρ_D calculated using Eq. (1) are fitted with Eqs. (3) and (4) to retrieve k_0 (attachment to the membrane), f (cooperativity) and k_2 (permeabilization).

4. Results and discussion

4.1. Antimicrobial activity of pepR

The methodology described above was used to study the killing of *E. coli* by pepR, a permeabilizing AMP [11]. The pepR concentration that inhibits 50% of bacterial growth (MIC_{50}) is 5 μM [11] (in agreement with Fig. 4A and Supplementary Section 1, Fig. S2). The antimicrobial activity of pepR was assayed against different *E. coli* strains (25922, K-12*wt* [12] and JW3596-1 [13]). Fig. 3 shows the effect of pepR (20 μM) on 25922 and K-12 *wt* over time (Supplementary Movies 1 and 2). In contrast, there is no effect of pepR on JW 3596-1 (Fig. 4 and Supplementary material Section 3, Fig. S3), a K-12*wt* mutant with a truncated LPS core [13]. The removal of LPS components from the bacterial surface abrogated permeabilization.

The kinetic data of pepR-induced permeabilization of 25922 and K-12 *wt* (Fig. 3) were fitted combining Eqs. (3) and (4). It should be stressed that the use of these equations follows the principle of parsimony: several kinetic models could in principle fit the data (e.g., Zeng et al. 2013 [22]) but the simplest is adopted (binding — local arrangement in the membrane — permeabilization). This formulation is in agreement with experimental data from different sources that shows that binding to membranes, accumulation in the membrane up to a critical level and subsequent permeabilization are events present in the mechanism of action of many AMP [4,6,23]. However, good fitting of the model to the data does not constitute definitive proof of such mechanism of action. k_0, f and k_2 are kinetic descriptors of permeabilization, not to be confused with literal phenomenological descriptors of the mechanism of action.

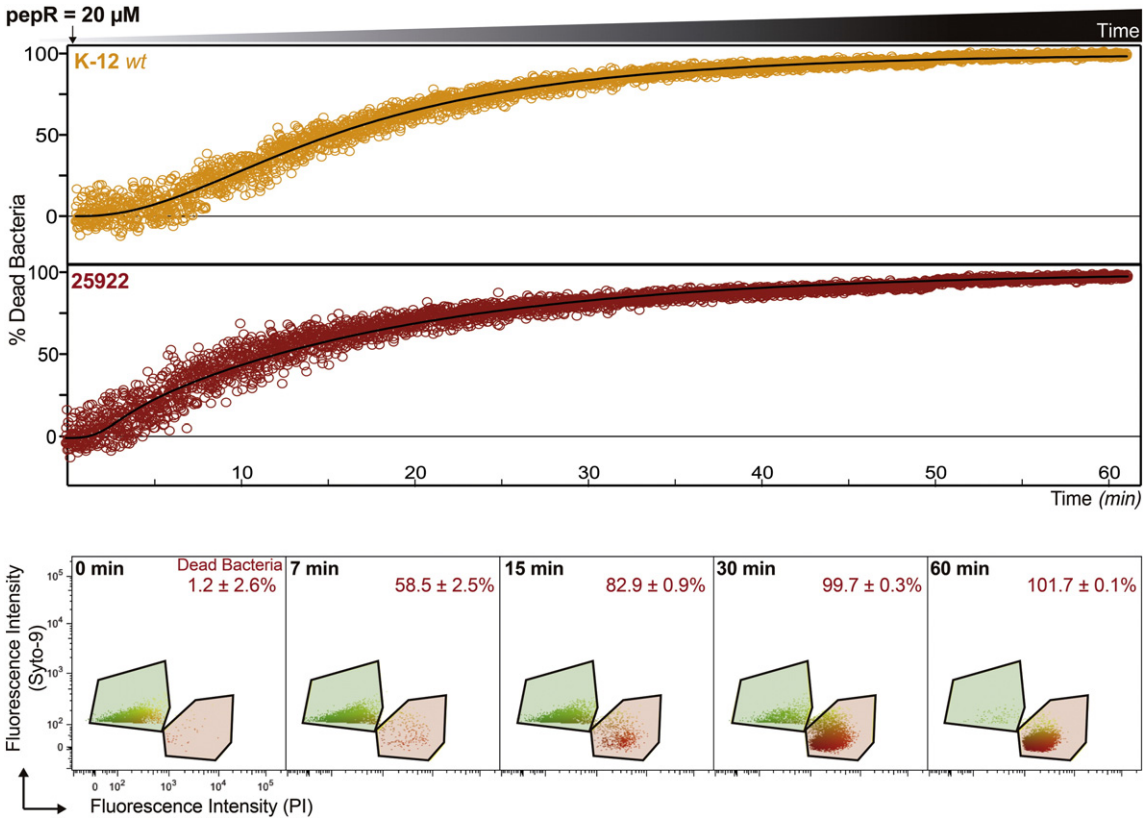

Fig. 3. Time-resolved bacterial damage of *Escherichia coli* ATCC 25922 and K-12 *wt* after addition of the permeabilizing antibiotic pepR. *Top panel:* Percentage of dead/permeabilized bacteria of K-12 *wt* (orange circles) and 25922 (red circles) over time after addition of 20 μM of pepR followed by time-resolved flow cytometry. The kinetics of bacterial permeabilization was fitted by Eq. (3) (black line), which is valid for a two-step process. *Bottom panel:* Flow cytometry fluorescence correlograms (PI *vs.* Syto-9) at specific time points during pepR antimicrobial action on 25922. Syto-9 and PI positive population gates (green and red, respectively) from which the percentage of dead bacteria is calculated be means of Eq. (1) are highlighted. For full observation of the result of the time-resolved flow cytometry experiment, see Supplementary Movies 1a, b and 2a,b before and after addition of 20 μM of pepR to 25922, respectively.

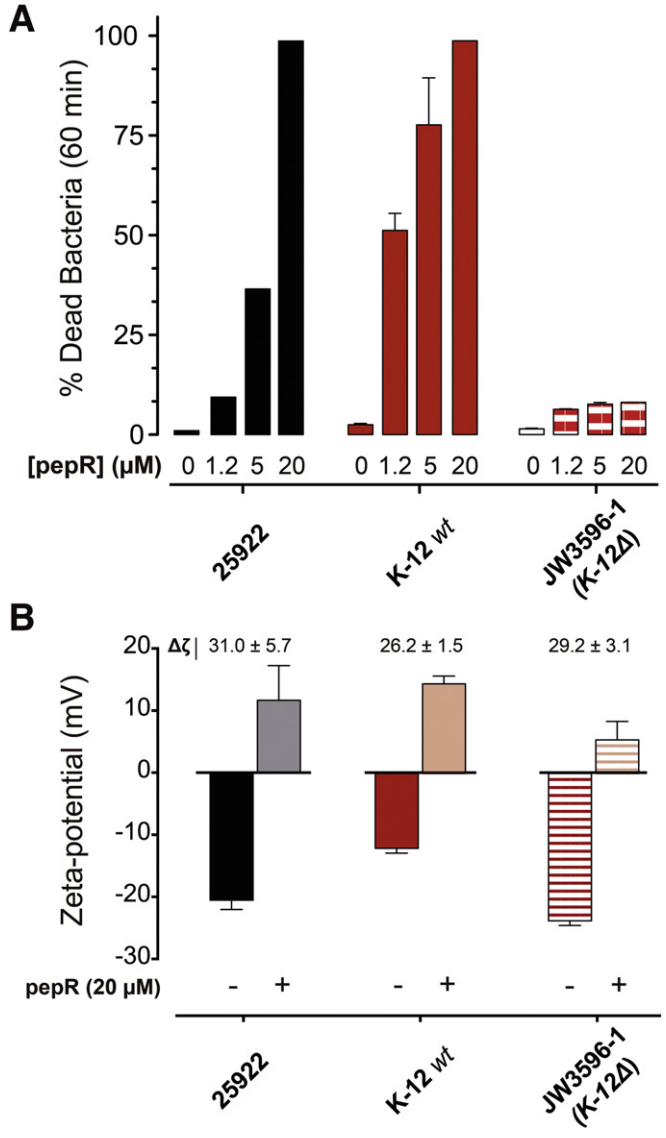

Fig. 4. pepR antimicrobial activity against Gram-negative bacteria. (a) Percentage of bacterial death and pepR concentration susceptibility for 25922, K-12*wt* and JW3596-1 after 60 min of incubation. Concentrations of pepR up to 20 μM (MIC_{50} = 5 μM [11]) were added to a bacterial suspension at 10^6 cfu/mL concentration doped with Syto-9 and PI. The Syto-9 and PI fluorescence signals were recorded after 1 h incubation (n = 3). (b) Zeta potential measurements of 25922 (black), K-12*wt* (red) and JW3596-1 (red stripes) in the absence and presence of 20 μM pepR. Bacteria were suspended in filtered HEPES buffer at 10^7 cfu/mL, dispensed into the disposable zeta cells and allowed to equilibrate for 15 min at 25 °C before measuring. The Zeta potential variation (Δζ) after addition of pepR is indicated. Error bars represent the standard deviation of at least three independent measurements.

The kinetic parameters reveal differences in the action of pepR toward 25922 and K-12 *wt* (Table 1 and Fig. 3). In light of the kinetic model used, pepR is more than 2-fold faster in binding to the membrane of 25922 , albeit being 40% slower than with K-12*wt* in the subsequent permeabilization step. Moreover, the antibiotic's cooperativity in binding to the bacterial membrane is more effective (higher *f*) for 25922 than K-12 *wt*. Binding to membranes is faster and highly cooperative in 25922 but the permeabilization step itself takes place at higher rate in K-12*wt*. It is reasonable to speculate that cooperativity probably results from aggregation in the membrane, because, as mentioned above, it is consensual in the literature that most cationic peptide antibiotics accumulate in the membranes until threshold critical levels are achieved [4,6].

Table 1
Kinetic parameters obtained from the non-linear fit of Eq. (4) to data from Fig. 3: time-resolved flow cytometry.

Kinetic parameters	*Escherichia coli* strains		
	25922	K-12 *wt*	Ratio (fold variation)
k_0 (min^{-1})	0.161 ± 0.045	0.071 ± 0.054	2.3
k_2 (min^{-1})	0.060 ± 0.0002	0.121 ± 0.015	0.6
f	1.44 ± 0.21	0. 60 ± 0.39	2.4

The kinetic data are consistent with results on the external surface charge density of each strain measured by zeta-potential [11] (Fig. 4B): −20 ± 2 mV for 25922, in agreement with published values [11,24], and −12,3 ± 0.4 mV for K-12 *wt*. These values show that it is possible that electrostatic attraction accounts for the dominant binding and clustering of the peptide in 25922 when compared with K-12*wt*. Interestingly, the subsequent step of permeabilization in the kinetic model is faster for K-12 *wt*. It is also worth to note that the JW 3596-1 zeta-potential value, −24 ± 1 mV, is similar to the one obtained for 25922 and binding to the membrane of these bacteria occurs (Fig. 4B) but permeabilization is nevertheless blocked. This reveals that the presence of negatively charged lipids compensates for the absence of LPS polysaccharide moieties in terms of surface membrane charge, but LPS has a crucial role in effective membrane permeabilization. Experimental evidence for the role of LPS in fusion of the outer and inner membranes leading to permeabilization has been presented before [25,26]. In addition, Avitabile et al. [27] reported by a direct study in bacteria that AMP secondary structure rearrangement is greatly dependent on LPS. Thus, it is possible that in bacteria with shorter LPS, the AMP may bind, but the secondary structure required for membrane disruption is not acquired.

In this work, we demonstrate the usefulness of time-resolved flow cytometry to study antibiotic-induced bacterial permeabilization. This technique enables to retrieve information on the kinetic efficacy of a permeabilizing agent and the cooperativity of its action. Gaining deeper insights on the kinetics of action of antibiotics will no doubt contribute to more rationally guided optimization, and eventually to more effective antimicrobial drugs with better clinical prospects.

5. Conclusions

There are few high-resolution methodologies to quantify the kinetics of antimicrobial permeabilization. This work presents a fast, reliable and accurate approach to retrieve kinetic parameters in the context of a simple model that considers antibiotic accumulation on the membrane followed by permeabilization. This methodology revealed that bacterial membrane LPS is important to the kinetics of AMP deleterious action. Structural in conjunction with kinetic data are needed to reveal the mechanism of action of AMPs, which has remained largely elusive, as biophysical studies using live cells are still minority compared to those using vesicles and artificial systems.

Supplementary data to this article can be found online at http://dx.doi.org/10.1016/j.bbamem.2014.11.001.

Competing financial interest

The authors have no competing financial interests.

Acknowledgements

We thank CGSC, Coli Genetic Stock Center, for the K-12 and JW3596-1 *Escherichia coli* strains. This work was supported by project PTDC/QUI-BIQ/112929/2009 from Fundação para a Ciência e a Tecnologia–Ministério da Educação e Ciência (FCT-MEC, Portugal). JMF and DG also acknowledge FCT-MEC for fellowships SFRH/BD/70423/2010 and SFRH/BPD/73500/2010, respectively, and ASV for funding within the FCT Investigator Programme (IF/00803/2012). Work at Pompeu Fabra University was supported by grants from the Spanish Ministry of

Economy and Competitiveness (SAF2011-24899) and from Generalitat de Catalunya (SGR2009-0492).

References

[1] M.R. Yeaman, A.S. Bayer, S.P. Koo, W. Foss, P.M. Sullam, Platelet microbicidal proteins and neutrophil defensin disrupt the Staphylococcus aureus cytoplasmic membrane by distinct mechanisms of action, J. Clin. Invest. 101 (1998) 178–187.
[2] D.J. Mason, F.C. Mortimer, V.A. Gant, Antibiotic susceptibility testing by flow cytometry, Curr. Protoc. Cytom. (2001) 1–11 (Chapter 11, Unit 11.8).
[3] M. Zasloff, Antimicrobial peptides of multicellular organisms, Nature 415 (2002) 389–395.
[4] M.N. Melo, R. Ferre, M.A.R.B. Castanho, Antimicrobial peptides: linking partition, activity and high membrane-bound concentrations, Nat. Rev. Microbiol. 7 (2009) 245–250.
[5] C.D. Fjell, J.A. Hiss, R.E.W. Hancock, G. Schneider, Designing antimicrobial peptides: form follows function, Nat. Rev. Drug Discov. 11 (2011) 37–51.
[6] K.A. Brogden, Antimicrobial peptides: pore formers or metabolic inhibitors in bacteria? Nat. Rev. Microbiol. 3 (2005) 238–250.
[7] A. Peschel, H.-G. Sahl, The co-evolution of host cationic antimicrobial peptides and microbial resistance, Nat. Rev. Microbiol. 4 (2006) 529–536.
[8] J.L. Fox, Antimicrobial peptides stage a comeback, Nat. Biotechnol. 31 (2013) 379–382.
[9] T. Ganz, Defensins: antimicrobial peptides of innate immunity, Nat. Rev. Immunol. 3 (2003) 710–720.
[10] G. Diamond, N. Beckloff, A. Weinberg, K.O. Kisich, The roles of antimicrobial peptides in innate host defense, Curr. Pharm. Des. 15 (2009) 2377–2392.
[11] C.S. Alves, M.N. Melo, H.G. Franquelim, R. Ferre, M. Planas, L. Feliu, E. Bardaji, W. Kowalczyk, D. Andreu, N.C. Santos, M.X. Fernandes, M.A.R.B. Castanho, *Escherichia coli* cell surface perturbation and disruption induced by antimicrobial peptides BP100 and pepR, J. Biol. Chem. 285 (2010) 27536–27544.
[12] T. Baba, T. Ara, M. Hasegawa, Y. Takai, Y. Okumura, M. Baba, K.A. Datsenko, M. Tomita, B.L. Wanner, H. Mori, Construction of *Escherichia coli* K-12 in-frame, single-gene knockout mutants: the Keio collection, Mol. Syst. Biol. 2 (2006) 2006. 0008.
[13] V. Chang, L.-Y. Chen, A. Wang, X. Yuan, The effect of lipopolysaccharide core structure defects on transformation efficiency in isogenic *Escherichia coli* BW25113 rfaG, rfaP, and rfaC mutants, J. Exp. Microbiol. Immunol. 14 (2010) 101–107.
[14] M. Berney, F. Hammes, F. Bosshard, H.U. Weilenmann, T. Egli, Assessment and interpretation of bacterial viability by using the LIVE/DEAD BacLight kit in combination with flow cytometry, Appl. Environ. Microbiol. 73 (2007) 3283–3290.
[15] S.M. Stocks, Mechanism and use of the commercially available viability stain, BacLight, Cytometry 61A (2003) 189–195.
[16] J.A. Lee, J. Spidlen, K. Boyce, J. Cai, N. Crosbie, M. Dalphin, J. Furlong, M. Gasparetto, M. Goldberg, E.M. Goralczyk, B. Hyun, K. Jansen, T. Kollmann, M. Kong, R. Leif, S. McWeeney, T.D. Moloshok, W. Moore, G. Nolan, J. Nolan, et al., MIFlowCyt: the minimum information about a flow cytometry experiment, Cytometry 73A (2008) 926–930.
[17] C.H. June, P.S. Rabinovitch, Flow cytometric measurement of intracellular ionized calcium in single cells with indo-1 and fluo-3, Methods Cell Biol. 33 (1990) 37–58.
[18] J.P. Nolan, L.A. Sklar, The emergence of flow cytometry for sensitive, real-time measurements of molecular interactions, Nat. Biotechnol. 16 (1998) 633–638.
[19] S.P. Perfetto, P.K. Chattopadhyay, M. Roederer, Seventeen-colour flow cytometry: unravelling the immune system, Nat. Rev. Immunol. 4 (2004) 648–655.
[20] C.A. Walshe, S.A. Beers, R.R. French, C.H.T. Chan, P.W. Johnson, G.K. Packham, M.J. Glennie, M.S. Cragg, Induction of cytosolic calcium flux by CD20 is dependent upon B Cell antigen receptor signaling, J. Biol. Chem. 283 (2008) 16971–16984.
[21] K.A. Connors, Chemical kinetics: the study of reaction rates in solution, VCH Publishers, New York, 1990.
[22] J. Zeng, H.M. Eckenrode, S.M. Dounce, H.-L. Dai, Time-resolved molecular transport across living cell membranes, Biophys. J. 104 (2013) 139–145.
[23] M.L. Gee, M. Burton, A. Grevis-James, M.A. Hossain, S. McArthur, E.A. Palombo, J.D. Wade, A.H.A. Clayton, Imaging the action of antimicrobial peptides on living bacterial cells, Sci. Rep. 3 (2013).
[24] I.M. Torcato, Y.-H. Huang, H.G. Franquelim, D.D. Gaspar, D.J. Craik, M.A.R.B. Castanho, S.T. Henriques, The antimicrobial activity of Sub3 is dependent on membrane binding and cell-penetrating ability, ChemBioChem 14 (2013) 2013–2022.
[25] M.M. Domingues, M.A.R.B. Castanho, N.C. Santos, rBPI21 promotes lipopolysaccharide aggregation and exerts its antimicrobial effects by (hemi)fusion of PG-containing membranes, PLoS ONE 4 (2009) e8385.
[26] M.M. Domingues, M.L. Bianconi, L.R.S. Barbosa, P.S. Santiago, M. Tabak, M.A.R.B. Castanho, R. Itri, N.C. Santos, Biochim. Biophys. Acta 1828 (2013) 2419–2427.
[27] C. Avitabile, L.D. D'Andrea, A. Romanelli, Circular dichroism studies on the interactions of antimicrobial peptides with bacterial cells, Sci. Rep. 4 (2014).